

The Nature of the Complex Counterion of the Chromophore in Rhodopsin

Minoru Sugihara,^{*,†} Volker Buss,^{*,‡} Peter Entel,[†] and Jürgen Hafner[§]

Theoretical Low-Temperature Physics, University of Duisburg-Essen, 47048 Duisburg, Germany,

Theoretical Chemistry, University of Duisburg-Essen, 47048 Duisburg, Germany, and

Center for Computational Materials Science, University of Vienna, 1090 Vienna, Austria

Received: August 4, 2003; In Final Form: November 10, 2003

The interaction of the rhodopsin chromophore with different complex counterions has been investigated using density functional theory methodology for both energy minimization and molecular dynamics calculations. The initial geometry of the retinal chromophore attached to Lys296 and of other amino acid residues close to the retinal binding site was taken from the rhodopsin X-ray structure by Palczewski et al. We also considered the presence of one water molecule (Wat2b) found in a recent study by Okada et al. The following counterions were studied (in order of increasing complexity): Glu113; Glu113 and Thr94; Glu113 and Wat2b; Glu113, Thr94, and Wat2b; Glu113, Thr94, Wat2b, and Cys187. With glutamate only, the protonated chromophore is not stable, and the proton is shifted rapidly to the glutamate counterion. Thr94 stabilizes the protonated chromophore by engaging the oxygen of Glu113 in hydrogen bonding. Wat2b works by the same mechanism, though the effect is weaker, and the chromophore oscillates between the protonated and the deprotonated state. The additional Cys187 does not change the essential features of this complex. The special stabilizing role of Thr94 is traced back to the stereochemical arrangement of the proton donor relative to Glu113.

1. Introduction

Rhodopsin is the pigment of retinal rod cells and mediates scotopic (light/dark) vision in the vertebrate eye. The chromophore of rhodopsin is 11-*cis*-retinal, which is connected to the apoprotein opsin via a protonated Schiff base linkage with Lys296. The visual process is started by photoisomerization of rhodopsin to bathorhodopsin which changes the chromophore configuration from 11-*cis* to all-*trans*.^{1,2} Subsequent conformational changes eventually lead to the activation of the intercellular surface of the protein toward coupling with the G-protein and initiation of the visual cascade.³ The initial photoisomerization is extremely fast, efficient, and selective: the photoproduct is formed within 200 fs⁴ with a quantum yield of 0.67,⁵ and only the C11–C12 bond is affected. These remarkable features, which are contingent on the retinal being bound to the protein, are the result of the specific interaction between the chromophore and the protein environment.

One peculiar aspect of the rhodopsin chromophore concerns its protonation state. In the ground (dark) state the retinal (Schiff base) is positively charged, with a salt bridge between the protonated Schiff base nitrogen and the negatively charged Glu113.^{6,7} The purple color of the protein results from the broad absorption band in the UV/vis spectrum, which peaks at 500 nm and is characteristic for the π -conjugated iminium salt.³ Because of conformational changes and/or changes of the protein environment, the absorbance of the chromophore is shifted by up to 70 nm toward the red (photorhodopsin) and 22 nm toward the blue (metarhodopsin I) in the ensuing intermediates. Upon

reaching the metarhodopsin II state, which is the last intermediate before the chromophore is released from the protein, a rather drastic change of the absorbance from 478 to 380 nm is observed. This blue shift is an indicator that the retinal Schiff base has become deprotonated^{8,9} and “one of the crucial stabilizing elements of the ground state of the protein is destroyed”.¹⁰ The factors that are responsible for the drop in the proton affinity of the chromophore from rhodopsin to metarhodopsin II are not known in detail. The first X-ray data of the ground-state structure of rhodopsin which have become available recently may provide an answer to part of this problem: what is the reason for the unusual stability of the protonated retinal Schiff base in the rhodopsin binding pocket where the pK_a is raised to a value possibly as high as 16?¹¹

The calculation of acid/base equilibria in proteins using classical electrostatic concepts has received considerable attention in the past two decades.^{12,13} On the basis of experimental protein structures and employing the finite difference solution of the Poisson–Boltzmann equation, several factors have been identified which contribute to the effective pK_a values of ionizable residues, among them the presence of charges, permanent and induced dipoles, and chemically bound water.^{14–16} For the specific interaction between a protein and a substrate which may lead to the stabilization of ionic transition states, the term “supersolvent” has been coined.¹⁷ It has been argued elsewhere¹⁸ that electrostatic preorganization of polar and polarizable groups is the key factor for solvating such an ionic state. This may be an apt description for the ground state of rhodopsin where the protonated chromophore acts as an inverse agonist against rhodopsin activation. We show that the binding pocket of rhodopsin can act as such a structurally organized supersolvent for stabilizing the chromophore ion pair though the “solvent” according to our calculations need not consist of more than two polar molecules.

[†] Theoretical Low-Temperature Physics, University of Duisburg-Essen.

[‡] Theoretical Chemistry, University of Duisburg-Essen.

[§] University of Vienna.

* Corresponding authors: e-mail minoru@thp.uni-duisburg.de, Fax +49-203-379-3665; e-mail theobuss@uni-duisburg.de, Fax +49-203-379-6110.

High-resolution diffraction structures of rhodopsin^{19–21} and efficient quantum-mechanical algorithms based on density functional theory (DFT) have become available in recent years, and so the study of retinal protein action at atomic resolution appears feasible. In our study we have combined quantum mechanics and X-ray structural data to elucidate the role of the complex counterion of the rhodopsin chromophore for regulating the equilibrium between the neutral form of the retinal chromophore and its protonated state. The rigorous nonempirical nature of these calculations limits the size of the system which can be treated. In addition to Glu113, whose role as the charged counterion of the Schiff base chromophore has been confirmed by the recent X-ray analyses, we have considered those ligands that can hydrogen-bind directly with Glu113 and thus can be expected to exert the largest influence on the relative stabilities of the states involved.

We find that in the presence of Glu113 the protonated chromophore is unstable and deprotonates spontaneously, transferring the proton to the glutamate ion. A water molecule (Wat2b) stabilizes the salt bridge somewhat, but a stronger effect is found when an additional amino acid, Thr94, which is close to the glutamate counterion, is added. By engaging the glutamate counterion in hydrogen bonding, this amino acid is able to inhibit the inherent tendency of the chromophore to deprotonate even in the absence of water. The effect is markedly enhanced in the presence of the water molecule. It has been shown by Fourier transform infrared spectroscopy that one or a few water molecules are located in the proximity of Glu113.^{22,23} However, Thr94 appears to have a definite advantage in comparison to Wat2b and can stabilize the protonation state of the chromophore more effectively. For a different view see ref 24. For Thr94 there are two slightly different coordinates in the literature.^{19,21} Both of them converge to an identical complex structure in which again the proton assumes a stable position close to the Schiff base nitrogen. The clue to the stabilizing effect of Thr94 is found in the relative orientation with respect to Glu113, which enables the amino acid to form an exceptionally strong hydrogen bond with the carboxylate group.²⁵

2. Computational Details and Model

DFT has developed into the method of choice for non-empirical molecular orbital calculations of large systems with inclusion of correlation energy. For our calculations we have employed two program packages, the Vienna ab initio simulation package (VASP), the description of which can be found in the literature,²⁶ and GAUSSIAN 98.²⁷ The VASP code is a program designed for ab initio quantum mechanical molecular dynamics (MD) simulations based on DFT. It uses Vanderbilt–Kresse ultrasoft pseudopotentials^{26,28} in a plane-wave basis set and performs a variational solution of the Kohn–Sham equations within the local density approximation (LDA) using the exchange–correlation functional of Perdew and Zunger²⁹ without or with the generalized gradient approximation (GGA).³⁰ The self-consistent calculation of the electronic ground state is performed using an iterative conjugate-gradient (CG) minimization of the one electron energy. The total energy is minimized by using the CG technique or alternatively by performing MD simulations. In MD use is made of the Born–Oppenheimer approximation, and the electronic wave function is optimized for any chosen nuclear configuration. The nuclei are treated as classical charged particles and then moved using the Hellmann–Feynman forces and the Verlet algorithm. VASP allows MD simulations as microcanonical or as canonical ensemble using the algorithm of Nosé.

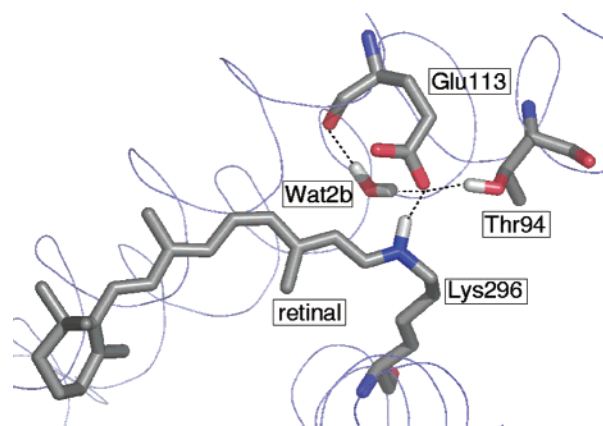


Figure 1. Energy-minimized structure of the chromophore binding site in rhodopsin consisting of protonated 11-*cis*-retinal Schiff base, Lys296, Glu113, Thr94, and Wat2b. The peptide backbone chains are truncated and were saturated with hydrogen atoms. Only the heavy atoms, three key hydrogen atoms, and the proton on the Schiff base are shown. The helices shown in the figure are parts of helices 2, 3, and 7. They are not included in our calculations.

The method has been applied with success to the study of many physical and chemical problems, such as liquid metals, clusters, hydrogen-bonded systems, chemical reactions, or chemisorption on surfaces, etc.^{31–33} For our calculations we employed periodic boundary conditions with a supercell of sufficient size ($28 \text{ \AA} \times 24 \text{ \AA} \times 24 \text{ \AA}$) to exclude the interaction with image molecules and one k point (Γ -point only). The size of the molecular fragment, 11-*cis*-retinal Schiff base with Glu113, Thr94, and Wat2b, is about $21 \text{ \AA} \times 11 \text{ \AA} \times 13 \text{ \AA}$. The cutoff energy of the plane wave basis was set 396.0 eV. All calculations are performed by using the GGA, a microcanonical ensemble, and a time step of 1.0 fs.

The starting geometries of the different chromophore/counterion complexes were taken from the rhodopsin coordinates laid down as 1F88 in the protein data bank.¹⁹ We used the coordinates of water (Wat2b) which is located close to Glu113 according to the most recent X-ray structure of rhodopsin.²¹ See Mizadegan et al.³⁴ for a discussion of these three structures. We considered the complete amino acids including their part of peptide backbone, $-\text{N}-\text{C}_\alpha-\text{C}-$, beyond which the bonds were cut. The remaining backbone chain was saturated where necessary with hydrogen atoms. Our minimal model system of the retinal binding site is charge neutral. If the retinal binding site were negatively charged for example by a deprotonated Glu181, it would probably stabilize the protonated Schiff base relative to the unprotonated one. However, according to experimental evidence both other glutamic acid residues near the chromophore (Glu122 and Glu181) are protonated,^{35,36} consistent with the results of two-photon spectroscopy.³⁷ Only the backbone atoms remained fixed during geometry optimization and the MD runs; everything else was allowed to move without constraints. The 11-*cis*-retinal chromophore inside the protein pocket is significantly twisted as the result of interaction with the protein.³⁸ The chromophore relaxes outside the protein pocket into a geometry that is essentially planar except for the C6–C7 bond. Previous calculations have shown that the planar structure of isolated 11-*cis*-retinal by VASP³⁹ is in good agreement with the results obtained with other quantum-chemical methods.^{40,41}

3. Results

3.1. Modeling the Binding Site. Figures 1 and 2 present the two largest complexes which we have studied. The structures

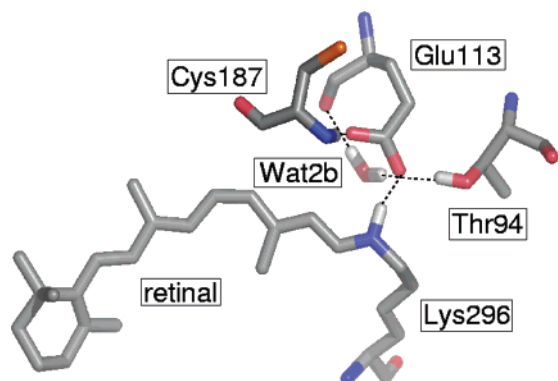


Figure 2. Energy-minimized structure of the chromophore binding site in rhodopsin consisting of protonated 11-*cis*-retinal Schiff base, Lys296, Glu113, Thr94, Wat2b, and Cys187.

have been energy-minimized subject only to the constraints listed above. The one shown in Figure 1 consists of the 11-*cis*-retinal chromophore attached to Lys296, Glu113, Thr94, and Wat2b. Only the heavy atoms, three key hydrogen atoms, and the proton on the Schiff base are shown in Figures 1 and 2. Analysis of the structure reveals that the Schiff base is protonated (distance between N and H⁺ 1.10 Å) and that there is a network of hydrogen bonds extending from the negatively charged glutamate to the Schiff base nitrogen (distance: 2.60 Å), to the threonine hydroxyl group (2.65 Å), and to Wat2b (3.14 Å). Wat2b makes a second hydrogen bond to the backbone oxygen of Glu113 (3.05 Å); the second oxygen of the glutamate carboxyl group is not coordinated because there is no ligand around.

In the second somewhat larger complex (Figure 2) Cys187 has been added. According to the crystal structure, this amino acid complexes via the peptide nitrogen atom with the second oxygen atom of Glu113. During the minimization process, we have also fixed the hydrogen atom connected to the Cys187 sulfur because in the protein it makes a disulfide bond with Cys110. The hydrogen bond network involving the retinal Schiff base proton is not affected by this change. Compared to the smaller complex, the structural changes are insignificant. The five distances quoted above which describe the hydrogen bond network are now 1.09, 2.63, 2.65, 3.15, and 3.04 Å, and the chromophore is still protonated. The distance between Glu113 oxygen and Cys187 nitrogen is 2.92 Å.

The similarity between the structures, especially the agreement between the bond lengths and dihedral angles, indicates that the major factors which bring about the protonation of the chromophore in the binding pocket of rhodopsin are accounted for already by the smaller of the two partial structures, i.e., the one depicted in Figure 1.

3.2. Energetics of Protonation. Using the methods of quantum chemistry, it is possible to analyze in detail the factors that are responsible for the stability of the protonated retinal Schiff base. By taking away stepwise components of the complex shown in Figure 1 and recalculating the energies of the proton attached either to the Schiff base or to the glutamate in the smaller complex, we have investigated how different compositions of the complex counterion affect the protonation equilibrium. The results based on restricted Hartree–Fock (RHF) theory with a 6-311G** basis set are presented graphically in Figure 3. Levels in the central box represent relative energies and correspond to complexes with (from the bottom) increasing complexity. Levels on the left in the box refer to the protonated chromophore, while on the right side the proton has been transferred from the chromophore to the glutamate anion.

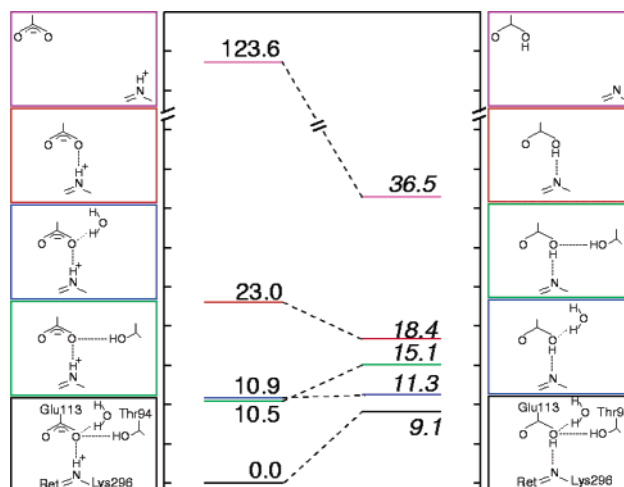


Figure 3. Relative energies (in kcal/mol) of the chromophore with different complex counterions. Energies correspond to single-point RHF/6-311G** calculations using VASP geometries. Levels on the left inside the central box correspond to the protonated state of the chromophore and levels on the right to the deprotonated state. The color codes correspond to the ones used in the MD simulations. Black is for the whole complex (Figure 1); green and blue refer to the complex without Wat2b and without Thr94, respectively. Red is for the complex of the chromophore and the counterion, and magenta refers to the system at infinite separation of the Schiff base and glutamate. Ret = N stands for the complete Schiff base chromophore. The complexes which we considered are schematically shown in the sideline boxes. All calculations are performed in vacuo. Note the interrupted energy scale between 50 and 100 kcal/mol.

Note that of all the levels plotted only the one at the bottom left corresponds to a truly energy-optimized geometry by VASP. All other energies result from single-point calculations, in which the relative orientation of the fragments after removal of a component or the transfer of the proton has been kept unchanged.

It is readily seen that with increasing complexity of the counterion (i.e., going down in the box) the relative stability of the retinal Schiff base/glutamic acid pair is gradually shifted from the right where the glutamic acid and the Schiff base are both neutral to the left in which the Schiff base is protonated and the ion pair is formed. The largest energy difference is calculated when no interaction between the two species is possible and amounts to 87.1 kcal/mol in favor of the neutral species. This value reflects the lower (gas phase) proton affinity of the retinal Schiff base relative to glutamate. Going down the figure we note the drastic stabilization of the charged complex, by more almost 100 kcal/mol, as the two species are brought into close contact. (The potential energy of two unit charges 2.5 Å apart is −132 kcal/mol.) The corresponding stabilization of the neutral species on the right side is considerably less, only 18.1 kcal/mol. As a result, the energies of the protonated Schiff base/glutamate ion pair and the neutral pair become comparable at this stage; however, the latter is still favored by 4.6 kcal/mol. Addition of Wat2b reverses the relative stabilities: the ion pair gains 12.1 kcal/mol, while the neutral couple benefits only by 7.1 kcal/mol. The effect of Thr94 is even larger than that of Wat2b; the corresponding numbers are 12.5 and 3.3 kcal/mol. The combined effect of Wat2b and Thr94 is almost additive, stabilizing the protonated retinal Schiff base by 9.1 kcal/mol against deprotonation. The color codes in Figure 3 correspond to the others used in the MD simulations in the following section.

The main features of these calculations are reproduced both with the hybrid DFT method (B3LYP with a 6-311G** basis

TABLE 1: Relative Energies (kcal/mol) Calculated by RHF/6-311G, B3LYP/6-311G**, and VASP for Different Complexities of the Counterion: 1, Complete Counterion; 2, without Wat2b; 3, without Threonine; 4, without Threonine and Wat2b; 5, Infinite Separation of the Schiff Base and Glutamate^a**

	1	2	3	4	5
RHF	0.0	10.5	10.9	23.0	123.6
	<i>9.1</i>	<i>15.1</i>	<i>11.3</i>	<i>18.4</i>	<i>36.5</i>
B3LYP	0.0	12.6	13.2	27.6	130.7
	<i>8.0</i>	<i>16.2</i>	<i>13.4</i>	<i>22.8</i>	<i>44.7</i>
VASP	0.0	9.9	12.3	23.7	<i>b</i>
	<i>9.6</i>	<i>15.7</i>	<i>14.9</i>	<i>22.1</i>	<i>44.3</i>

^a Plain numbers correspond to the charged ion pair and numbers in italics to the neutral pair. ^b Not available due to limitation of the method.

set) and with VASP (Table 1): the strong bias toward deprotonation of the Schiff base when the proton acceptor glutamate is far away, the significant stabilization of the ion pair at experimental distance making it comparable in energy with the neutral couple, and the effects of Wat2b and the significantly larger effect of Thr94. For the entire counterion the agreement is almost quantitative, 8.0 (B3LYP/6-311G**), 9.1 (RHF/6-311G**), and 9.6 kcal/mol (VASP) in favor of the ion pair.

3.3. Watching the Proton Move: MD Simulations. A more realistic description of the interaction between the retinal Schiff base and the different complex counterions is obtained from MD simulations. MD avoids the pitfalls of local minima as a result of the usual CG geometry optimization procedures, an important feature especially in complicated systems with many degrees of internal freedom. Also, since only the entire complex has been geometry-optimized but not the fragments shown in Figure 3, it is desirable to complete the study by unfreezing these structures. Of special interest will be to see how the acidic proton reacts to the presence of two competing basic sites, the Schiff base on the one and the glutamate ion on the other.

Figures 4–6 give an account of the MD simulations that were performed. The colors correspond to the different complex counterions and show how the proton reacts to the changes in the environment. The color code is identical to the one used in Figure 3; thus, black corresponds to the complete complex; green and blue indicate removal of Wat2b and Thr94, respectively, and in red both are removed, leaving only the glutamate counterion.

The minimization of the total energy of the system consisting of the chromophore with three amino acid residues and Wat2b was performed with MD by simulated annealing for 200 fs (Figure 4, in black). The temperature of the optimizing MD run reaches about 12 K. The wiggling line in the center reflects the vibration of the bridging hydrogen atom. The average distance to the Schiff base nitrogen is 1.10 Å and to the glutamate oxygen is 1.50 Å; i.e., the chromophore is clearly protonated under these conditions. Running the MD simulation of the same complex starting with the bridging proton closer to the glutamate ion immediately shifts the proton to the Schiff base nitrogen atom where it stays. There is no barrier separating the protonated and deprotonated states of chromophore, and we conclude that the deprotonated Schiff base does not exist at this level of complexity.

200 fs into the simulation of the complex two parallel MD runs were started by removing either Wat2b or Thr94. Without Wat2b the structure and the dynamics of the complex are essentially unchanged; the chromophore remains protonated, though the hydrogen amplitudes are increasing somewhat. Without threonine the changes are more distinct. The hydrogen

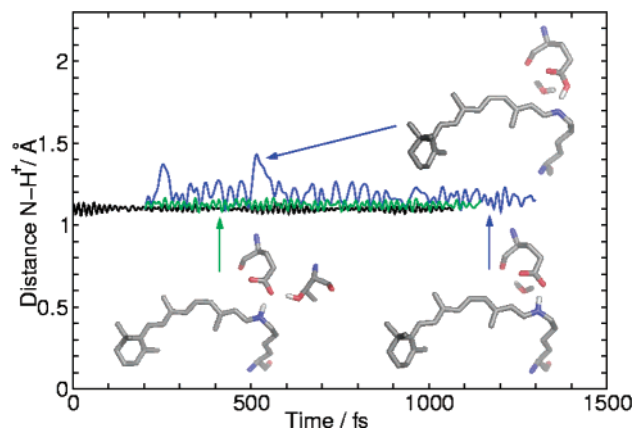


Figure 4. MD simulation of the complete complex (in black) and the effect of removing either Thr94 (in blue) or Wat2b (in green). The “distance” is measured between the Schiff base nitrogen and the proton. Insets depict complexes and the position of the acidic hydrogen.

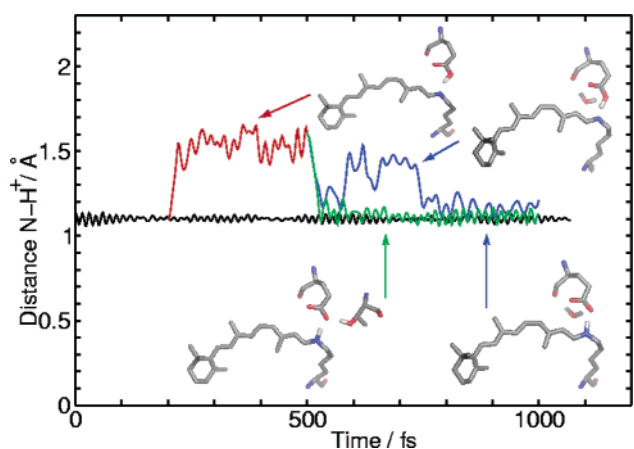


Figure 5. MD simulation of the complete complex (in black) and the effect of removing both Thr94 and Wat2b from the complex (in red) and putting back Wat2b (in blue) or Thr94 (in green).

starts to oscillate strongly, with the distance to the glutamate oxygen reaching values as low as 1.0 Å. However, in the end the hydrogen settles at the Schiff base nitrogen again.

Figure 5 shows what happens when Wat2b and Thr94 are removed from the complex and then inserted back again separately. Upon removing the two components, the proton is shifted immediately toward the glutamate ion, and the chromophore becomes deprotonated. The large amplitude of the proton vibrational motion is exaggerated; if the vibration of the oxygen atom is taken into account, the oscillations appear rather smooth. 500 fs into the simulation threonine (in green) or Wat2b (in blue) is inserted back into the complex, and the MD is restarted from 1 K. With threonine the Schiff base is rapidly protonated, and the proton motion is very similar to the one observed in the complete complex. The average distance increases slightly, from 1.10 to 1.11 Å (average of the 800 to 1000 fs time), and shows that Wat2b is not necessary to effect protonation of the chromophore if threonine is present. With Wat2b the picture is different. The proton shifts first to the nitrogen, then bounces back toward the oxygen, and only after 250 fs, and after the excess energy has dissipated, it settles down on the Schiff base again. Both the reduced frequency of the N–H⁺ vibration and the enlarged amplitude indicate that the hydrogen bond is significantly weaker than in the presence of threonine. Also, the N–H⁺ distance of 1.17 Å (average value between 800 and 1000 fs) is larger than in the presence of threonine.

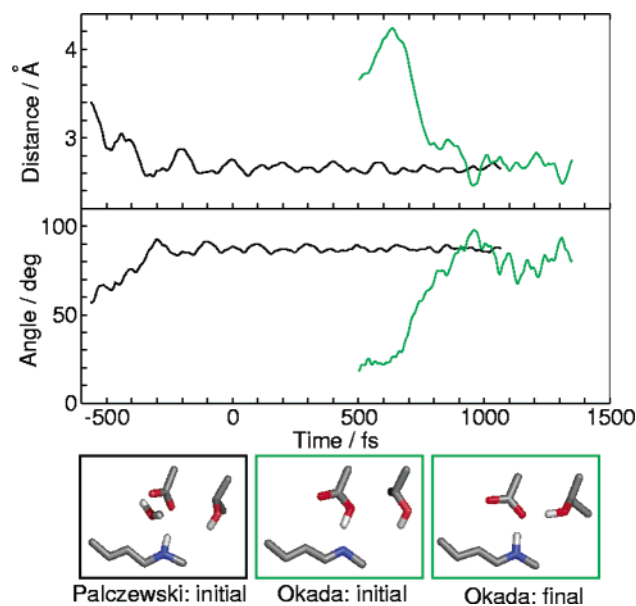


Figure 6. MD simulation using the Okada threonine geometry. The figure shows the distance between O_γ of Thr94 and oxygen of Glu113 (top) and the dihedral angle, $C-\alpha-C_\beta-O_\gamma$ of Thr94 (bottom). After rotating and making hydrogen bond with Glu113, the chromophore is reprotonated.

The deprotonation of the retinal Schiff base chromophore in the absence of Wat2b and Thr94 and the reprotonation in the presence of either Wat2b or Thr94 closely correspond to the energetics of the protonation equilibrium discussed in the preceding section.

To clarify the possible involvement of Cys187 in stabilizing the protonated chromophore, we have removed both Thr94 and Wat2b from the energy-optimized structure of Figure 2 and find that the protonation state changes quickly, with the proton moving immediately to the glutamate. We conclude that the basicity of the glutamate is not reduced sufficiently by the hydrogen bond of Cys187 to prevent the deprotonation of chromophore.

Finally we have followed the motion of Thr94 when it is inserted in the complex according to the data reported by Okada²¹ (Figure 6). The Okada Thr94 geometry differs from the one proposed by Palczewski¹⁹ mainly in the orientation of the side chain relative to the backbone: whereas in the latter the OH group is close to the Schiff base nitrogen and the methyl group points away from the glutamate, the methyl group is close to the oxygen atom of Glu113 in the Okada structure.

The two black curves in Figure 6 trace the geometry optimization of the Palczewski structure starting with the initial geometry of 1F88 (simulated annealing up to 0 fs, then MD). They correspond to the distance between the Glu113 carboxylate oxygen and the Thr94 hydroxyl oxygen and the $C_\alpha-C_\beta$ dihedral angle of Thr94. Geometry optimization involves significant dihedral adjustment of the Thr94 side chain, until the hydrogen bond with Glu113 is formed and the dihedral angle is fixed. The MD calculations clearly show that except for the torsional motion of the Thr94 side chain the Palczewski geometry is stable. This is the geometry that was used as the point of departure for the experiments shown in Figures 4 and 5.

For the MD calculations based on Okada's structure Wat2b and Thr94 are removed from the equilibrated Palczewski structure at 200 fs, resulting in a deprotonated chromophore. Then, Thr94 according to Okada is put back in at 500 fs (green curves in Figure 6). Because of steric repulsion by the methyl group, the distance between Thr94 and Glu113 increases

initially, until the terminal group of threonine starts to rotate and the hydrogen bond with Glu113 is formed. The final geometries of the Okada and Palczewski structures are virtually identical, though they start from significantly different orientations of the threonine side chain as measured by the $C-C_\alpha-C_\beta-O_\gamma$ dihedral angles: Palczewski, 57°; Okada, 17°; equilibrated structure, 86°.

Both Cys185 and Gly90 can hydrogen-bind to the Thr94 OH group via the amide oxygen backbone according to the two recent QM/MM studies.^{42,43} To study this possibility, we added these two residues to the complex shown in Figure 2 according to the Palczewski structure. The size of the molecular fragment is about 23 Å × 17 Å × 17 Å, so we chose a somewhat larger supercell (32 Å × 28 Å × 28 Å); all other simulation parameters were left unchanged. The Thr94 hydroxyl oxygen is 3.4 Å from the backbone oxygen of Cys185 and from the carboxylate oxygen of Glu113. For the starting geometry we formed a hydrogen bond between Thr94 and Cys185 and studied the stability of the complex by MD. After an induction period of some 30 fs the Thr94 OH group starts to oscillate between Cys185 and Glu113, with the distance to the latter slowly decreasing. This movement is accompanied by strong fluctuation of the Schiff base proton. After 200 fs the new hydrogen bond between Thr94 and Glu113 is formed, and the proton settles on the Schiff base again.

4. Discussion

Controlling the protonation state of the retinal chromophore in rhodopsin is of crucial importance for the visual process. The free base is nonpolar, with essentially localized double bonds much like the parent aldehyde, and an absorption centered around 357 nm (methanol). Protonation shifts the absorption maximum into the visible region, a consequence of significant double-bond delocalization. Also, the delocalized positive charge renders the system highly sensitive toward the external charge distribution, an effect which is vital for spectral tuning and color vision: absorbances of different rhodopsins with retinal or similar systems as chromophores range from 360 to 630 nm.⁴⁴ How the protein affects this control is not clear at all; however, the recent X-ray analysis of the binding site has clarified the situation somewhat.

In the presence of a carboxylic acid (pK_a around 2) the equilibrium is far to the side of the protonated retinal (pK_a of 7.5 in methanol/water⁴⁵). In the protein and thus in the absence of water on which the stabilization of both charged species depends things are more complicated, and protonation of the basic amino group is not a foregone conclusion. Glycine which offers both protonation sites in one molecule does not appear to exist in the zwitterionic state in the gas phase.⁴⁶ This agrees with calculations at the MP2-corrected RHF/DZP level⁴⁷ that neutral glycine is more stable than the zwitterionic structure. Which then are the factors that stabilize the charged ion pair in rhodopsin?

Sheves, who has performed competitive titration studies and concludes that the acid strength of the retinal chromophore in rhodopsin is raised by as many as 16 pK_a units,¹¹ lists two mechanisms which significantly affect the pK_a of the protonated Schiff base: (i) the distance between the positively charged polyene and the carboxylate counterion; (ii) hydrogen bonding to the carboxylate and the bipolar groups, including water molecules. The influence of water in the binding site has been pointed out in several studies.⁴⁷⁻⁴⁹

Our calculations corroborate this proposal. The key to understanding the interplay between the chromophore and the

different components of the complex counterion is the molecular architecture of the binding site shown in Figure 1. The accuracy of the theoretical model of the binding site exceeds the experimental resolution by far. However, with the MD simulations of the two large complexes shown in Figures 1 and 2 and the Okada variant all converging to the same equilibrium geometry, we feel we are not overinterpreting the data when we point at the following structural peculiarities of the binding site. These are (i) the very short hydrogen bond between the nitrogen and the Glu113 carboxylate group and (ii) the very peculiar arrangement of two potential proton donors, the extra Wat2b and Thr94.

The calculated energies of different scenarios (Figure 3 and Table 1) show very clearly that in the absence of bulk water there is only one possibility to make protonation of the Schiff base competitive against charge neutralization, and that is the intimate contact between the two charged species. At the calculated N—H \cdots O distance of 2.60 Å, the energy difference favoring the neutral pair has shrunk from 87.1 to 4.6 kcal/mol (RHF data). This enormous stabilization of the charged ion pair is caused by two effects: localization of the positive charge of the chromophore on the nitrogen, as indicated by a significant increase of bond alternation in going from the free protonated Schiff base to the ion pair,³⁸ and the gain in Coulomb attraction as the two charges are brought together. With less than 5 kcal/mol energy difference the equilibrium between the charged and the neutral couple is easily shifted by secondary interactions, such as stabilization of the glutamate counterion by hydrogen bonding to Wat2b or Thr94.

Both the MD simulations and the single-point calculations indicate that of the two Thr94 is more effective in stabilizing the protonated chromophore. The hydrogen bond network near the Schiff base shows why this is the case. With its planar structure and the lone pair electron lobes disposed at 120° with respect to the C—O bond a proton donor can approach the plane of the carboxylate group either in the preferred syn or in the anti configuration.⁵⁰ The Schiff base nitrogen is in the favored position: the N—H bond is planar-syn; the deviation from the COO[−] plane is only 2°. The Thr94 hydroxyl group is in the second best position: anti but with significant deviation, 35°, from the COO[−] plane. With both lone electron pairs occupied, the only way for Wat2b to access the carboxylate oxygen is from out-of-plane (the O—C—O \cdots H—O dihedral is 78°, i.e., almost perpendicular). With 3.14 Å this hydrogen bond is significantly larger than the Thr94 hydrogen bond (2.65 Å), which is an indication that in this orientation Wat2b is the weaker hydrogen donor.

Stabilizing the protonated Schiff base by an amino acid side chain rather than by one or two appropriately placed water molecules has obvious advantages. Water molecules are mobile and will follow charges wherever they go. When the position of the hydrogen donor is fixed, the protein can control the protonation state by simply changing the disposition of the Schiff base nitrogen relative to the counterion, e.g., by a conformational change of the chromophore. While this may not be operative in the early stages of the visual transduction process, it may be later when deprotonation is actually required to reach the activated state of the protein.

Thr94 residue is highly conserved in rhodopsin pigments.⁵¹ There are experimental indications that Thr94 affects the protonation state of the rhodopsin chromophore. Thr94Ile is one of only three mutations known to cause congenital stationary night blindness (CSNB) in humans,⁵² and it has been argued that similar to the two other mutants^{53,54} which involve residues

close to the retinal binding site replacement of Thr94 by the nonpolar isoleucine might affect the salt bridge and destabilize the Schiff base/glutamate ion pair.^{55–57} Of the two alternatives offered as an explanation—hydrogen bonding of Thr94 with water or with Glu113—our calculations clearly favor the latter. Whether the observed 22 nm blue shift in the absorption of the mutant is due to the increased hydrophobicity of isoleucine compared to threonine or reflects the weakened hydrogen bond between the Schiff base and Glu113 remains, however, to be seen. On the other hand, the mutation Thr94Ser shows the same stability as wild-type rhodopsin.⁵⁶ This is understandable because serine, like threonine, has a polar OH group, which could stabilize the protonated chromophore.

The other mutation, Gys90Asp, was found to slow the rate of the Schiff base formation in opsin.^{54,58} Our MD simulation has shown that Cys185 and Gly90 do not affect the hydrogen bond network around the counterion. However, switching the hydrogen bond of Thr94 from Glu113 to the aspartic acid at the position 90 might easily cause the chromophore to deprotonate.

In a recent paper,²⁴ Yamada et al. have performed QM/MM calculations on the rhodopsin chromophore including what they consider to be the essential amino acid residues. They conclude that Ser186 and Cys187 play a significant role in stabilizing the protonated state of the chromophore. According to their results, Thr94 cannot stabilize the protonated Schiff base. At the RHF/6-31G* level they calculate that the energy of the protonated Schiff base/glutamate ion pair with threonine is 1.34 kcal/mol higher than that of the neutral pair with threonine. Our single-point calculations of the optimized geometry have shown that the ion pair is more stable in the presence of threonine (RHF/6-311G**: 4.6 kcal/mol; VASP: 5.8 kcal/mol; see Table 1). The single-point VASP calculations with threonine in the Okada geometry (but without Wat2b) show that the effect of threonine is weaker (1.1 kcal/mol), probably on account of the hydrogen bond which is not being formed. However, the presence of Thr94 is still sufficient to stabilize the protonated Schiff base. We assume that in the geometry calculated by Yamada et al. Thr94 does not form a hydrogen bond with Glu113. However, the exact orientation of the counterion, especially the distance to the positive nitrogen, is also crucial in these calculations.

Breaking the salt bridge between the Schiff base and the counterion activates the G-protein, although available methods do not answer the question whether the proton that leaves the chromophore and the one that neutralizes Glu113 are identical.⁵⁹ One possibility is that changing the direct hydrogen bond as well as the distance between the counterion and the Schiff base makes the protonated state unstable. An alternative has been proposed recently by Yan et al.,⁶⁰ who have obtained experimental evidence that the Schiff base counterion switches from Glu113 to Glu181 during the photoactivation of rhodopsin. According to this scenario, neutralization of the counterion involves a fundamental change of the binding site. One related problem concerns the violet cone pigments, which have an unprotonated Schiff base, although they contain a threonine residue at the same position as rhodopsin.⁶¹ As the electrostatic energy gain is very sensitive to the distance of ion pairs, it is not surprising that this short wavelength absorbing pigment can support an unprotonated Schiff base even in the presence of a polar residue. For a more quantitative discussion, one would need three-dimensional crystal structures of the resolution achieved for rhodopsin.

5. Conclusion

With the main goal of studying the factors affecting the protonation state of the 11-*cis*-retinal Schiff base chromophore inside the protein binding pocket of rhodopsin, a model for the binding site of the chromophore has been developed using nonempirical quantum-theory only. On the basis of X-ray structural data of the protein which have become available recently, we find that a geometry-optimized model consisting of Lys296 with the chromophore attached, Glu113 as the charged counterion, and Thr94 and Wat2b as supplementary hydrogen donors suffices to reproduce the remarkable fact that the chromophore is stable against deprotonation in this nonpolar environment. The stability is traced back to the geometry of the binding site: the strong hydrogen bond between the Schiff base nitrogen and glutamate in an almost ideal arrangement and the additional involvement of the other supplementary groups in an extended hydrogen-bond network. Our calculations show that of these two Thr94 is essential to lower the basicity of Glu113 and protect the chromophore against deprotonation. MD simulations reveal several possibilities for a switching mechanism where the removal or change of the geometric disposition of one of the two supplementary groups induces rapid proton transfer from the chromophore to the glutamate counterion.

The possible involvement of other polar side chains close to the chromophore binding site has been studied: Cys187 which hydrogen binds to the second glutamate oxygen does not change the geometry of the complex; we presume that its effect on the dynamics of the protonation can likewise be neglected. Cys185 and Gly90 might bind to Thr94 and thereby limit the effectiveness of the latter to stabilize the protonated Schiff base. Our calculations show that this is not the case and that Thr94 prefers coordination with Glu113 even in the presence of these two groups.

Warshel, in a recent article on computer simulations of enzyme action,⁶² has warned against possible pitfalls of these calculations, especially when applying high-quality ab initio calculations to a necessarily small part of the enzyme and neglecting the influence of the enzyme as a whole. While these warnings may be justified in general and especially to transition states which are structurally poorly defined, rhodopsin appears to present a different case. The substrate—the protonated chromophore—enjoys a specific stabilization inside the binding pocket leading to a well-defined constrained structure quite different from the solution structure. This stabilization is crucial for the “exceedingly low activity of rhodopsin”¹¹ and the resulting high barrier against thermal noise. The calculations we have presented for the retinal binding site account for these (structural) constraints. It is gratifying to note that they can account for vital electronic effects of the type reported here as well.

Acknowledgment. This work was supported by the Research Group on Molecular Mechanisms of Retinal Protein Action at the Universities of Paderborn, Heidelberg, and Duisburg-Essen and by the Graduate School on Structure and Dynamics of Heterogeneous Systems at the University of Duisburg-Essen, both financed by the German Research Council. All computations were performed at the Computational Center of the University of Duisburg-Essen and at the Regional Computer Center of the University of Cologne.

References and Notes

- (1) Yoshizawa, T.; Wald, G. *Nature (London)* **1963**, 197, 1279.
- (2) Wald, G. *Science* **1968**, 162, 230.
- (3) Hubbard, R.; Kropf, A. *Proc. Natl. Acad. Sci. U.S.A.* **1958**, 44, 130.
- (4) Schoenlein, R. W.; Peteanu, L. A.; Mathies, R. A.; Shank, C. V. *Science* **1991**, 254, 412.
- (5) Dartnall, H. J. A. *Vision Res.* **1967**, 8, 339.
- (6) Zhukovsky, E. A.; Oprlan, D. D. *Science* **1989**, 246, 928.
- (7) Nathans, J. *Biochemistry* **1990**, 29, 9746.
- (8) Doukas, A. G.; Aton, B.; Callender, R. H.; Ebrey, T. G. *Biochemistry* **1978**, 17, 2430.
- (9) Cohen, G. B.; Oprin, D. D.; Robinson, P. R. *Biochemistry* **1992**, 31, 12592.
- (10) Okada, T.; Ernst, O. P.; Palczewski, K.; Hofmann, K. P. *Trends Biochem. Sci.* **2001**, 26, 318.
- (11) Steinberg, G.; Ottolenghi, M.; Sheves, M. *Biophys. J.* **1993**, 64, 1499.
- (12) Sharp, K. A.; Honig, B. *Annu. Rev. Biophys. Biophys. Chem.* **1990**, 19, 301.
- (13) Yang, A. S.; Gunner, M. R.; Sampogna, R.; Sharp, K.; Honig, B. *Proteins* **1993**, 15, 252.
- (14) Sampogna, R. V.; Honig, B. *Biophys. J.* **1994**, 66, 1341.
- (15) Birge, R. R. *Biochim. Biophys. Acta* **1990**, 1016, 293.
- (16) Spassov, V. Z.; Luecke, H.; Gerwert, G.; Bashford, D. *J. Mol. Biol.* **2001**, 312, 203.
- (17) Warshel, A. *Proc. Natl. Acad. Sci. U.S.A.* **1978**, 75, 2558.
- (18) Warshel, A.; Barboy, N. *J. Am. Chem. Soc.* **1982**, 104, 1469.
- (19) Palczewski, K.; Kumasaka, T.; Hori, T.; Behnke, C. A.; Motoshima, H.; Fox, B. A.; Le Trong, I.; Teller, D. C.; Okada, T.; Stenkamp, R. E.; Yamamoto, M.; Miyano, M. *Science* **2000**, 289, 739.
- (20) Teller, D. C.; Okada, T.; Behnke, C. A.; Palczewski, K.; Stenkamp, R. E. *Biochemistry* **2001**, 40, 7761.
- (21) Okada, T.; Fujiyoshi, Y.; Silow, M.; Navarro, J.; Landau, E. M.; Shichida, Y. *Proc. Natl. Acad. Sci. U.S.A.* **2002**, 99, 5982.
- (22) Nagata, T.; Terakita, A.; Kandori, H.; Kojima, D.; Schichida, Y.; Maeda, A. *Biochemistry* **1997**, 36, 6164.
- (23) Nagata, T.; Terakita, A.; Kandori, H.; Schichida, Y.; Maeda, A. *Biochemistry* **1998**, 37, 17216.
- (24) Yamada, A.; Kakitani, T.; Yamamoto, S.; Yamato, T. *Chem. Phys. Lett.* **2002**, 366, 670.
- (25) A preliminary account of this work has recently been published: Buss, V.; Sugihara, M.; Entel, P.; Hafner, J. *Angew. Chem., Int. Ed.* **2003**, 42, 3245.
- (26) Kresse, G.; Furthmüller, J. *Phys. Rev. B* **1996**, 54, 11169.
- (27) Gaussian 98 (Revision A.1): Frisch, M. J.; Trucks, G. W.; Schlegel, H. B.; Scuseria, G. E.; Robb, M. A.; Cheeseman, J. R.; Zakrzewski, V. G.; Montgomery, J. A.; Stratmann, R. E.; Burant, J. C.; Dapprich, S.; Millam, J. M.; Daniels, A. D.; Kudin, K. N.; Strain, M. C.; Farkas, O.; Tomasi, J.; Barone, V.; Cossi, M.; Cammi, R.; Mennucci, B.; Pomelli, C.; Adamo, C.; Clifford, S.; Ochterski, J.; Petersson, G. A.; Ayala, P. Y.; Cui, Q.; Morokuma, K.; Malick, D. K.; Rabuck, A. D.; Raghavachari, K.; Foresman, J. B.; Cioslowski, J.; Ortiz, J. V.; Stefanov, B. B.; Liu, G.; Liashenko, A.; Piskorz, P.; Komaromi, I.; Gomperts, R.; Martin, R. L.; Fox, D. J.; Keith, T.; Al-Laham, M. A.; Peng, C. Y.; Nanayakkara, A.; Gonzalez, C.; Challacombe, M.; Gill, P. M. M.; Johnson, B. G.; Chen, W.; Wong, M. W.; Andres, J. L.; Head-Gordon, M.; Replogle, E. S.; Pople, J. A. *Gaussian, Inc., Pittsburgh, PA*, 1998.
- (28) Vanderbilt, D. *Phys. Rev. B* **1990**, 41, 7892.
- (29) Perdew, J. P.; Zunger, A. *Phys. Rev. B* **1981**, 23, 5048.
- (30) Perdew, J. P.; Chevary, J. A.; Vosko, S. H.; Jackson, K. A.; Pederson, M. R.; Singh, D. J.; Fiolhais, C. *Phys. Rev. B* **1992**, 46, 6671.
- (31) Benco, L.; Tugega, D.; Hafner, J.; Lischka, H. *J. Phys. Chem. B* **2001**, 105, 10812.
- (32) Meyer, H.; Entel, P.; Hafner, J. *Surf. Sci.* **2001**, 488, 177.
- (33) Rozanska, X.; van Santen, R. A.; Hutschka, F.; Hafner, J. *J. Am. Chem. Soc.* **2001**, 123, 7655.
- (34) Mirzadegan, T.; Benkö, G.; Filipek, S.; Palczewski, K. *Biochemistry* **2003**, 42, 2759.
- (35) Fahmy, K.; Jäger, F.; Beck, M.; Zvyaga, T. A.; Sakmar, T. P.; Siebert, F. *Proc. Natl. Acad. Sci. U.S.A.* **1993**, 90, 10206.
- (36) Yan, E. C.; Kazmi, M. A.; De, S.; Chang, B. S. W.; Seibert, C.; Martin, E. P.; Mathies, R. A.; Sakmar, T. P. *Biochemistry* **2002**, 41, 3620.
- (37) Birge, R. R.; Murray, L. P.; Pierce, B. M.; Akita, H.; Balogh-Nair, V.; Finsen, L. A.; Nakanishi, K. *Proc. Natl. Acad. Sci. U.S.A.* **1985**, 82, 4117.
- (38) Sugihara, M.; Buss, V.; Entel, P.; Elstner, M.; Frauenheim, T. *Biochemistry* **2002**, 41, 15259.
- (39) Sugihara, M.; Entel, P.; Meyer, H.; Buss, V.; Terstegen, F.; Hafner, J. *Prog. Theor. Phys. Suppl.* **2000**, 138, 107.
- (40) Terstegen, F.; Buss, V. *J. Mol. Struct. (THEOCHEM)* **1996**, 369, 53.
- (41) Terstegen, F.; Buss, V. *J. Mol. Struct. (THEOCHEM)* **1998**, 430, 209.
- (42) Röhring, U. F.; Guidoni, L.; Rothlisberger, U. *Biochemistry* **2002**, 41, 10799.

- (43) Saam, J.; Tajkhorshid, E.; Hayashi, S.; Schulten, K. *Biophys. J.* **2002**, *83*, 3097.
- (44) Schichida, Y.; Imai, H. *Cell. Mol. Life Sci.* **1998**, *54*, 1299.
- (45) Gat, Y.; Sheves, M. *J. Am. Chem. Soc.* **1993**, *115*, 3772.
- (46) Ding, Y.; Krogh-Jespersen, K. *Chem. Phys. Lett.* **1992**, *199*, 261.
- (47) Jensen, J.; Gordon, M. S. *J. Am. Chem. Soc.* **1995**, *117*, 8159.
- (48) Harosi, F. I.; Sandorfy, C. *Photochem. Photobiol.* **1995**, *61*, 510.
- (49) Hudson, B. S.; Birge, R. R. *J. Phys. Chem. A* **1999**, *103*, 2274.
- (50) Glusker, J. P. *Top. Curr. Chem.* **1998**, *198*, 1.
- (51) Yokoyama, S.; Yokoyama, R. Comparative Molecular Biology of Visual Pigments. In *Handbook of Biological Physics*; Stavenga, D. G., DeGrip, W. J., Pugh, E. N., Jr., Eds.; Elsevier Science Press: Amsterdam, The Netherlands, 2000; Vol. 3, p 257.
- (52) al-Jandal, N.; Farrar, G. J.; Kiang, A. S.; Humphries, M. M.; Bannon, N.; Findlay, J. B. C.; Humphries, P.; Kenna, P. F. *Human Mutation* **1999**, *13*, 75.
- (53) Rao, V. R.; Cohen, G. B.; Oprian, D. D. *Nature (London)* **1994**, *367*, 639.
- (54) Dryja, T. P.; Berson, E. L.; Rao, V. R.; Oprian, D. D. *Nat. Genet.* **1993**, *4*, 280.
- (55) Garriga, P.; Manyosa, J. *FEBS Lett.* **2002**, *528*, 17.
- (56) Ramon, E.; del Valle, L. J. Garriga, P. *J. Biol. Chem.* **2003**, *278*, 6427.
- (57) Gross, A. K.; Rao, V. R.; Oprian, D. D. *Biochemistry* **2003**, *42*, 2009.
- (58) Gross, A. K.; Xie, G.; Oprian, D. D. *Biochemistry* **2003**, *42*, 2002.
- (59) Hofmann, K. P. Late Photoproducts and Signaling States of Bovine Rhodopsin. In *Handbook of Biological Physics*; Stavenga, D. G., DeGrip, W. J., Pugh, E. N., Jr., Eds.; Elsevier Science Press: Amsterdam, The Netherlands, 2000; Vol. 3, p 91.
- (60) Yan, E. C.; Kazumi, M. A.; Ganim, Z.; Hou, J. M.; Pan, P.; Chang, B. S. W.; Sakmar, T. P.; Mathies, R. A. *Proc. Natl. Acad. Sci. U.S.A.* **2003**, *100*, 9296.
- (61) Dukkipati, A.; Kusnetzow, A.; Babu, K. R.; Ramos, L.; Singh, D.; Knox, B. E.; Birge, R. R. *Biochemistry* **2002**, *41*, 99842.
- (62) Warshel, A.; Parson, W. W. *Q. Rev. Biophys.* **2001**, *34*, 563.